Camera position and posture estimation from a still image using feature landmark database

Tomokazu Sato, Yoshiyuki Nishiumi, Mitsutaka Susuki, Tomoka Nakagawa and Naokazu Yokoya[1]

[1]Nara Institute of Science and Technology, 8916-5 Takayama, Ikoma-shi, Nara, 630-0192 Japan
(E-mail: tomoka-s@is.naist.jp)

Abstract: Several human navigation services are currently available on the cellular phones that uses embedded GPS and 2-D map. However, 2-D map based human navigation is not always easy to understand for users because that is not intuitive. In order to realize more intuitive human navigation, AR (Augmented Reality) based navigation where guiding information is overlaid in the real image is expected to be the next generation navigation system. For AR navigation, the key problem is how to acquire the accurate position and posture of the embedded camera on the cellular phone. Many researchers have intensively tackled to the camera parameter estimation problem for AR in recent years. However, most of these methods cannot be applied to the current mobile devices because they are designed to treat video sequence where temporal information like camera parameter of the previous frame is known. In this research, we propose a novel method that estimates camera parameters of single input image using SIFT features and voting scheme.

Keywords: user localization, extrinsic camera parameter estimation, landmark database.

1. INTRODUCTION

Several human navigation services are currently available on the cellular phones that uses embedded GPS and 2-D map. However, 2-D map based human navigation is not always easy to understand for users because that is not intuitive. In order to realize more intuitive human navigation, AR (Augmented Reality) based navigation where guiding information is overlaid in the real image is expected to be the next generation navigation system. For AR navigation, the key problem is how to acquire the accurate position and posture of the embedded camera on the cellular phone. Many researchers have intensively tackled to the camera parameter estimation problem for AR in recent years. However, most of these methods cannot be applied to the current mobile devices due to several problems.

In order to realize AR-based navigation system on the consumer mobile devices, at least, following four requirements should be satisfied.

(1) Equipment should be simple.
(2) Method should work in various environments.
(3) 6-DOF position and posture should be estimated.
(4) Computational cost should be low.

In the following paragraphs, conventional localization methods are categorized and their problems are pointed out based on above requirements.

The conventional methods for localization of mobile devices can be categorized into two groupes; the sensor-based approach [1-3] and the image-based approach [4-11]. Sensor-based approach uses combination of several sensors to acquire both position and posture parameters. Since most of these methods rely on GPS, the raw accuracy of the position given by the embedded GPS on mobile devices is 10 m order and it is not sufficient to realize AR navigation. Although there is possibility to acquire high accurate position and posture by combining several sensors such as RTK-GPS, optical fiber gyro, and magnetic sensors, combined equipment is complex and it is not suitable for mobile devices.

Image-based approach uses captured images to estimate camera position and posture parameters. Methods in this approach can be categorized into four groups; (a) Marker-based methods that use number of artificial markers and their 3-D positions [4, 5], (b) methods based on image retrieval that estimate camera position and posture by searching the image database for similar image [6, 7], (c) model-based methods where position and posture parameters are determined in such a way that the visibility of the 3-D model becomes similar to the input image [8, 9], (d) landmark-based methods that use pre-registered 3-D points of image features instead of the artificial markers [10, 11]. All these methods can estimate position and posture parameters of a camera without sensors by using pre-constructed database that models the target environment or object. Thus, equipment of the mobile device can be small and simple in the case the image-based approach is employed.

However, each group in the image-based approach still has problems to realize AR navigation on mobile devices. In the marker-based method (a), the problem is cost for marker arrangement and maintenance. It is almost impossible to set up and maintain the artificial markers in large outdoor environments. Methods based on image retrieval (b) cannot estimate 6-DOF position and posture parameters because its image database does not contain 3-D data for target environment. The model-based method (c) also has a problem that construction of accurate 3-D model for a complex and large environment is difficult. On the other hand, landmark-based method (d) does not have such problems. In the landmark-based method, 3-D database for an environment is constructed automatically by applying structure-from-motion method to the video sequences that capture the target environment. By using a high-resolution omnidirectional camera, a large number

of feature landmarks in the target environment can be effectively collected and registered to the feature landmark database. After database construction, camera position and posture are estimated by using corresponding pairs of feature points and landmarks.

The landmark-based method potentially satisfies all the requirements (1) to (4) in the case we employ the server-client scheme where the client (mobile device) captures a still image and camera parameter estimation is processed on the server. Although this approach suits the current cellular phones, most of the conventional methods assume video sequence as an input. Because the video sequence easily consumes the bandwidth of the network and computational resources, the conventional works could not be applied for the mobile devices. Instead of the video sequence, we select a still image as an input. To apply the landmark-based approach for a still image input, we must develop the method that can find correct correspondences without good initial parameters for camera position and posture.

In this paper, based on the feature landmark database, we propose a novel method that can estimate 6-DOF extrinsic camera parameters from a still image input. As shown in Figure 1, our method is constructed of two phases. In the offline phase, the landmark database is developed by applying structure from motion to the omnidirectional video streams. In the online phase, to find the correct correspondences from a large number of visually similar landmarks, we gradually discard the candidates of landmarks. First, rough position of the user (100m order accuracy is assumed) given by the embedded GPS or the strength of the electric waves of the mobile phone is used to select the database from a mount of landmark database that may be developed in every site of the world. Next, visually similar landmarks with the image features on the input image are selected using SIFT descriptor and LoG based scale detector. In this process, uniqueness in each landmark is used as priority of matching order to reduce computational matching cost. Spatially consistent landmarks are then selected by voting approach for camera position and posture. Finally, 6-DOF camera position and posture are estimated by solving PnP problem with RANSAC based outlier elimination.

This paper is organized as follows. In Section 2, we describe the first phase of our method, which specifies the construction of the feature landmark database. Section 3 describes the position and posture estimation method for a still image using the feature landmark database. Section 4 shows the experimental results in an outdoor environment, and Section 5 summarizes this paper.

2. DATABASE CONSTRUCTION

Before camera parameter estimation for mobile devices, feature landmark database must be constructed for the target environment where localization service will be provided. Basically, the feature landmark database is constructed by 3-D positions of feature points and their visual information. In the following sections, first, elements of feature landmark database are described. The way of database construction is then detailed.

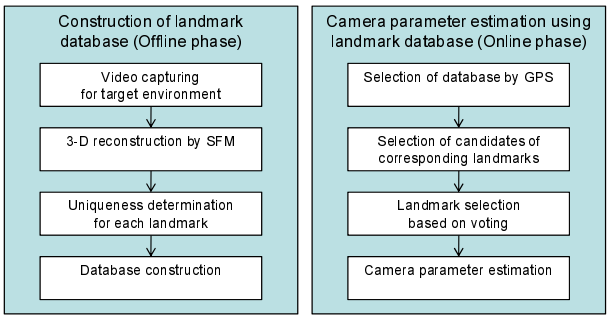

Fig. 1 Flow diagram of proposed method.

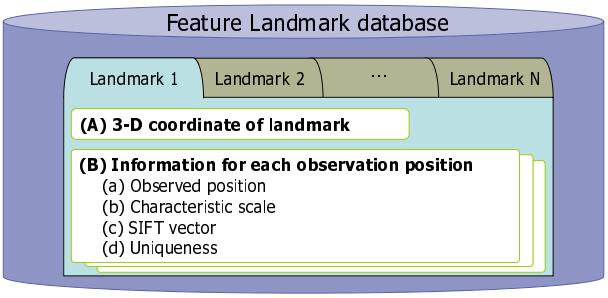

Fig. 2 Elements of feature landmark database.

2.1 Elements of Feature Landmark Database

As shown in Figure 6, feature landmark database consists of a number of landmarks. Each landmark retains the 3-D coordinate of itself (A), and several information acquired from different observation positions (B). Information for different observation positions consists of four elements: (a) observed position, (b) characteristic scale, (c) SIFT vector, (d) Uniqueness of landmark pattern. In the offline phase, these elements are acquired by analyzing video images that captures the target environment.

2.2 3-D reconstruction for environment

The target environment is captured as video sequences at first. In this paper, moving an omnidirectional multi-camera system is assumed to be used as a scanner for the target environment. For the acquired video sequences, structure from motion method for multi-camera system [12] is applied to estimate 3-D positions of feature points and camera parameters. In the method [12], image features detected by Harris operator [13] are tracked trough the input video sequences and 3-D positions of image features and camera parameters of the camera system are estimated based on the bundle adjustment [14]. It should be noted that general structure from motion cannot recover the absolute 3-D position and scale by itself and all the recovered 3-D positions are relative. To arrange the recovered 3-D points for an absolute coordinate, some control points of known 3-D positions should be given to the bundle adjustment process [12], or hybrid approach should be employed that uses both motion of image features and absolute positions measured by GPS attached with the camera system [15]. In the experiment that is

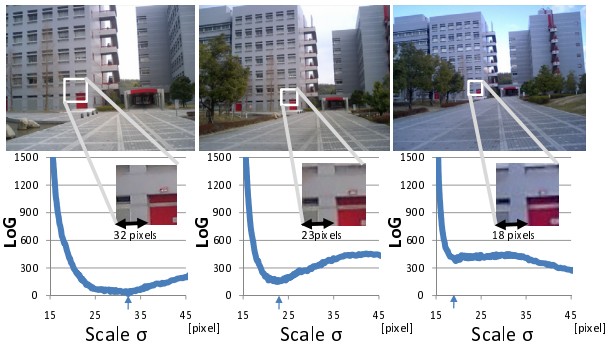

Fig. 3 Determination of characteristic scale by Laplacian of Gaussian.

described in Section 4, the former approach has been employed.

2.3 Determination of characteristic scale and SIFT vector

In this research, in order to achieve rotation and distortion invariant matching, SIFT [16] is employed as feature descriptor. Although SIFT includes characteristic scale determination scheme that uses DoG (Difference of Gaussian), in this paper, we have employed LoG (Laplacian of Gaussian) instead of DoG because DoG is used as an approximation of LoG in the article [16] and LoG based scale detector is compatible with Harris detectors that is used as feature detector in the structure from motion process [17].

To remove visual changes depending on camera posture and lens distortion, first, all the acquired images by the omnidirectional multi-camera system are warped to the sphere whose radius is infinite. Next, for each image feature whose 3-D position is estimated, characteristic scale is determined by using LoG function. As shown in Figure 3, responses of the LoG function for different images become similar in the case there exists same image structure. Thus, characteristic scale is determined by searching for scale parameter σ that maximizes the LoG value for the image feature on the sphere. The LoG value is computed by applying LoG filter to the image on the sphere. The LoG filter is defined as follows:

$$f(r,\sigma) = -\frac{r^2 - 2\sigma^2}{2\pi\sigma^6}\exp(-\frac{r^2}{2\sigma^2}), \tag{1}$$

where the scale parameter σ is identical to the radius of this filter and r is a distance from the center of the filter to the target pixel. After characteristic scale is determined, image pattern inside of the circle whose radius is σ and center is the position of the feature point is coded by SIFT descriptor [16].

2.4 Determination of uniqueness

Generally, there exist visually similar landmarks in an environment. Because these un-unique landmarks easily correspond to incorrect image features, unique landmarks are preferentially corresponded to the image features in this research.

In order to select unique landmarks, the uniqueness E_i for the landmark i is computed by using SIFT distances of N-top nearest landmarks as follows.

$$E_i = \frac{1}{N}\sum_{k=1}^{N} |\mathbf{f}_i - \mathbf{f}_{\mathbf{h}_{ik}}| \tag{2}$$

where $\mathbf{f}_i$ is the D-dimensional SIFT vector of the landmark i. $\mathbf{h}_i$ is an index list for the landmark i in which the index of the landmark is sorted in ascending order of the SIFT distance to the landmark i: $\mathbf{h}_{ik}$ indicates the index of k-th nearby landmark from the landmark i in the SIFT space.

3. CAMERA PARAMETER ESTIMATION USING LANDMARK DATABASE

In this section, the processes for the online phase are described. In this research, we assume that the feature landmark database constructed by the offline phase is stored in the server and all the processes described in this section are carried out in the server. To estimate the camera position of the client, the server needs both an input image and rough position that is measured by embedded GPS or strength of electric waves from cellular phones. The rough position is necessary to select the appropriate database from a mound of database for every site. After landmark selection by GPS, SIFT vectors and characteristic scales for image features on the input image are computed by the same manner with the landmark construction process. Unique landmarks are then selected and corresponded with image features. Un-unique landmarks are also corresponded using roughly estimated camera parameters using unique landmarks. Spatially consistent landmarks are then selected by voting for observable position and posture for corresponded landmarks. Finally, camera position and posture are estimated by solving PnP problem with RANSAC based outlier elimination. Following paragraphs describes these processes.

3.1 Correspondence for unique landmarks

For the feature points detected in the input image, firstly, unique landmarks are preferentially corresponded. Because unique landmarks do not have similar landmarks in the target environment, rate for incorrect correspondences for these landmarks is lower than that for un-unique landmarks. Unique landmarks are corresponded with image features by following processes.

(1) Most unique landmark in the landmarks that are not selected until the current iteration is selected.

(2) The SIFT distance between the selected unique landmark and each feature point j in the input image is computed as the squared distance between SIFT vector $\mathbf{f}_{\mathbf{LM}_p}$ of the landmark i and $\mathbf{f}_{\mathbf{IN}_j}$ of the feature point j:

$$S_p(j) = |\mathbf{f}_{\mathbf{LM}_p} - \mathbf{f}_{\mathbf{IN}_j}|^2, \tag{3}$$

In this step, the feature point j_m that minimize $S_p(j)$ is selected. In the case $S(j_m)$ is under given threshold, the feature point j_m is selected as corresponding point for the landmark p, otherwise the landmark p

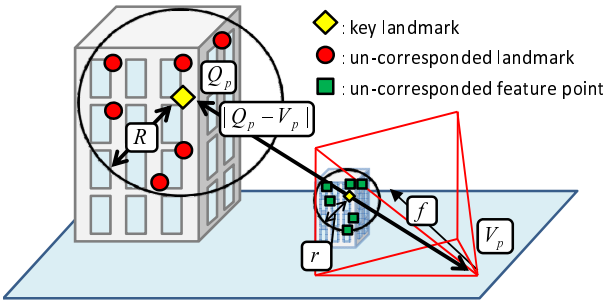

Fig. 4 Limitation of matching candidates using key landmarks.

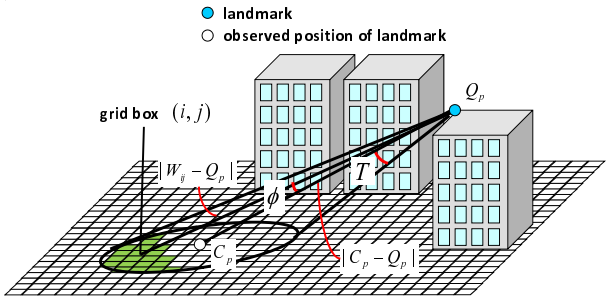

Fig. 5 Voting from a landmark.

is not corresponded to any image features and the process returns to the step (1).

(3) By the landmark p that is corresponded to the feature point j_m, the camera position $\mathbf{V}_p$ from where the landmark p can be visible as the feature point j_m is computed. $\mathbf{V}_p$ is determined by following equation using 3-D position $\mathbf{Q}_p$ of the landmark p, the position $\mathbf{C}_p$ from where the landmark p is captured, the characteristic scale ω_p and ω_{shoot} for the landmark and feature point j_m.

$$\mathbf{V}_p = \mathbf{Q}_p - \frac{\omega_p}{\omega_{shoot}}(\mathbf{Q}_p - \mathbf{C}_p). \quad (4)$$

(4) For all the positions $\mathbf{V}_n (n \neq p)$ that is computed until the current iteration, the number of the position $\mathbf{V}_n$ that satisfy $|\mathbf{V}_p - \mathbf{V}_n| < K (K$ is a given threshold) is counted.

(5) If the counted number becomes M or more, the landmarks that satisfy $|\mathbf{V}_p - \mathbf{V}_n| < K$ are selected as key landmarks and the other landmarks are discarded as outliers.

3.2 Correspondence for un-unique landmarks

By using the corresponded key landmarks and image features, the rest of the image features and un-unique landmarks are effectively corresponded by limiting spatial searching range. Concretely, as shown in Figure 4, first, in the 3-D space, the landmarks that exist inside the sphere of radius R whose center is the 3-D position $\mathbf{Q}_p$ of the key landmark p are selected. Similarly, on the image plane, image features that exist inside the circle of radius r whose center is the 2-D position of the feature j_m that is corresponded to the key landmark p are selected. The SIFT distances for these selected landmarks and image features are computed and corresponding pairs are determined as the same manner with the method described in the previous section. The radius R is computed by following equation.

$$R = \frac{r}{f}|\mathbf{Q}_p - \mathbf{V}_p|, \quad (5)$$

where f is a focal length of the camera.

3.3 Landmark selection based on voting

The corresponding pairs of landmarks and feature points that are selected in the previous step still include a lot of outliers. In this step, outliers are eliminated by verifying the space consistency based on the fact that the input image is captured from a unique position and a unique posture. To verify the space consistency, we employ the voting approach.

As illustrated in Figure 5, the ground plane around the roughly specified client position is divided into $(2h+1) \times (2h+1)$ grid boxes. Each grid box has l ballot boxes that are for horizontal orientation. Each landmark throws a vote for the m-th ballot box at the grid (i, j); $(-h \leq i \leq h, -h \leq j \leq h)$ if the box satisfies following two conditions.

Angular condition: The angle ϕ is under threshold T. ϕ is the angle of following two lines; (Line 1) the line connecting 3-D position $\mathbf{Q}_p$ of the landmark p and the observed position $\mathbf{C}_p$ for the landmark p, (Line 2) the line connecting $\mathbf{Q}_p$ and the position $\mathbf{W}_{ij} = (w_i, w_j, c_z)$ where w_i, w_j are the horizontal position of the grid box (i, j) and c_z is altitude element of $\mathbf{C}_p$.

Scale condition: The ratio of the characteristic scale ω_p of the landmark p and the characteristic scale ω_q of the corresponding image feature q on the input image is agree with the distance ratio of $|\mathbf{W}_{ij} - \mathbf{Q}_p|$ and $|\mathbf{C}_p - \mathbf{Q}_p|$: $1 - \alpha < \frac{\omega_p |\mathbf{W}_{ij} - \mathbf{Q}_p|}{\omega_q |\mathbf{C}_p - \mathbf{Q}_p|} < 1 + \alpha$ (where α is a threshold).

The ballot box m at the grid (i, j) is determined by $m = [\theta l / 2\pi]$ where $[a]$ returns the integer value of a, and θ is the horizontal angle (radian) between the x-axis and the vector $\mathbf{W}_{ij} - \mathbf{Q}_p$. After voting from all the landmarks, the landmarks that vote for the box of maximum count are selected. These selected landmarks are considered to be visible from a unique position and a unique posture. However position and posture can be determined by (w_i, w_j) and θ in this step, they are still 3-DOF and they cannot be used for AR navigation. Next section describes how to upgrade these parameters to 6-DOF.

3.4 6-DOF extrinsic camera parameter estimation

In this step, by using selected landmarks in the previous step, 3-DOF camera position and posture are upgraded to 6-DOF. By using the 3-DOF parameters as initial parameter, the re-projection errors are minimized with non-linear optimization. The re-projection error is defined by distances between 2-D position of feature point on the input image and projected position of the 3-D position of the corresponding landmark. To remove outliers from the selected landmarks, in this process, we

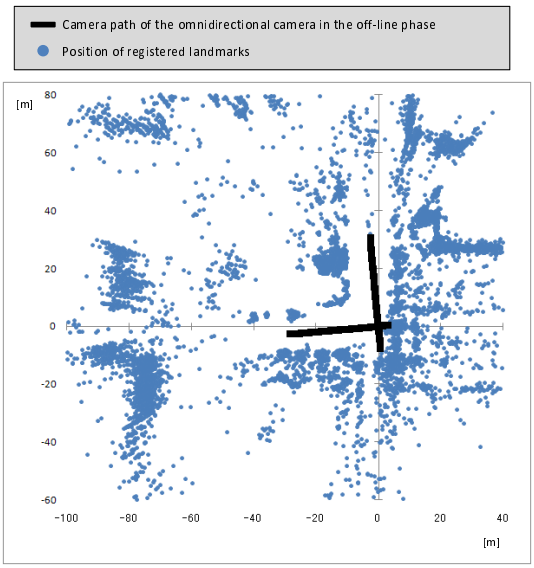

Fig. 6 Position of registered landmarks and omnidirectional camera for database construction.

employ RANSAC approach that can be used when outliers are fewer than inliers.

It should be noted that after final estimation result is given, the system can judge the validity of the estimated camera parameter based on the re-projection errors. In this research, if an average re-projection error is larger than the given threshold E, the system judges that the estimated result is not accurate.

4. EXPERIMENT

To show the validity of the proposed method, the feature landmark database is actuary constructed for a real outdoor environment and the accuracy of camera position and posture by the proposed method is evaluated by comparing it with the ground truth. In this experiment, first, we have captured the target environment as two omnidirectional video sequences by using an omnidirectional multi-camera system (Pointgrey Ladybug) that has six camera units of XGA resolution. In this experiment, about 12,500 landmarks are registered to the database. Each input image is taken as VGA sized digital photograph from the 6×6 positions that are arranged by the 5m grid using the digital camera embedded in the cellular phone (CASIO GzOne W42CA). In this environment, we take images for two directions. For direction 1, buildings that contains many landmarks are visible from most of the positions as shown in Figure 7(a). In contrast, for direction 2, buildings are blinded by trees from many positions as shown in Figure 7(b).

In this experiment, although server-client system is assumed, the prototype system has not been developed yet. Thus, input images were once stored into the mobile phone and camera position and posture for each image were estimated after all photographs were taken. Table 1 shows thresholds that are used in this experiment. The ground truth of the camera position and postures are given by solving PnP problem using manually specified

(a) Sampled input images for direction 1.

(b) Sampled input images for direction 2.

Fig. 7 Sampled input images.

correspondences for landmarks and image features. For 7 of 72 images, we cannot compute the ground truth due to lack of visible landmarks and thus we didn't use these 7 images for this evaluation. Thus, we have evaluated with 65 images whose ground truths are available.

Table 2 shows success rate of estimation and average and standard deviation of estimation errors. Figure 8 illustrates judged results for each input. For direction 1, except the positions where trees severely blind buildings, most of estimated results is judged as successful by the system. As shown in Table 2, average position error and posture error are 0.7 m and 0.8 degree and it is considered as sufficient level for AR navigation. For direction 2, for more than half positions, estimated result was judged as failed (re-projection error was over 5 pixels). For these images, even when enough number of landmarks are visible in the input image, most of correct landmarks had been rejected because image patterns around landmarks on the buildings are overlaid by branches of trees and they affect characteristic scale determination. To realize more stable estimation for various environments, introduction of more robust ways for characteristic scale determination and corresponding point detection is necessary. For the environment where landmarks are hardly detected, user interactive scheme is also one of the solutions where the system suggests good directions for landmark detection based on the current estimation.

5. CONCLUSION

In this paper, we propose novel method for extrinsic camera parameter estimation using a still image and feature landmark database that contains multi-dimensional and multi-view data. In this method, feature landmark database is constructed in advance by using structure

Table 1 Parameters that is used in experiment.

Dimension for SIFT vector	128
Angle threshold T (degree)	10
Scale ratio threshold α	0.2
Maximum re-projection error E (pixel)	5.0
Threshold K for key landmark selection (m)	5.0
Threshold M for key landmark selection	6

Table 2 Success rate and accuracy of estimated results.

	Dir. 1	Dir. 2
Success rate of estimation (%)	68.9	52.7
Average position error (m)	0.7	2.8
Std.dev. position error (m)	0.5	4.3
Average posture error (deg.)	0.8	1.2
Std.dev. posture error (deg.)	0.5	1.9
Average re-projection error (pix.)	2.1	2.2
Std.dev. re-projection error (pix.)	1.0	3.9

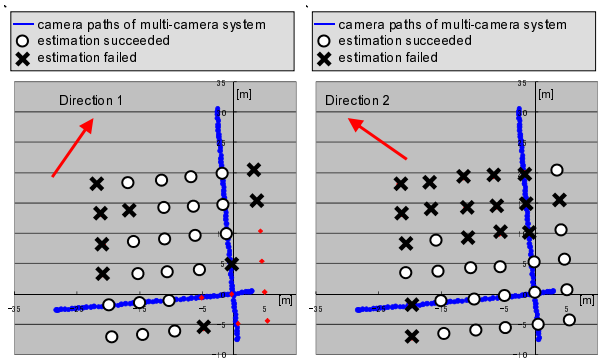

(a) for direction 1 (b) for direction 2

Fig. 8 Succeeded and failed positions for each direction.

from motion method for video sequences that capture the target environment. From the registered landmarks, corresponding points of image features in the input image are searched by gradually limiting candidates. Finally, 6-DOF camera position and posture are estimated by using pairs of image features and landmarks. By the experiment, the accuracy of the position and posture estimation are reached to the level that AR navigation can be realized on the mobile devices. However, for the environment where most of the scene is covered by nature, it is difficult to estimate the position and posture stably. In the future work, robustness for camera parameter estimation will be improved by investigating robust scale determination and matching for occluders. User interactive scheme will also be explored to develop more useful system.

Acknowledgment: This paper is supported by SCOPE (Strategic Information and Communications R&D Promotion Programme) of Ministry of Internal Affairs and Communication Japan.

REFERENCES

[1] S. Feiner, B. MacIntyre, T. Höller and A. Webster: "A touring machine: Prototyping 3d mobile augmented reality systems for exploring the urban environment,", Proc. Int. Symp. on Wearable Computers (ISWC 1997), pp. 74–81, 1997.

[2] T. Höllerer, S. Feiner and J. Pavlik: "Situated documentaries: Embedding multimedia presentations in the real world,", Proc. Int. Symp. on Wearable Computers (ISWC 1999), pp. 79–86, 1999.

[3] R. Tenmoku, M. Kanbara and N. Yokoya: "A wearable augmented reality system using positioning infrastructures and a pedometer,", Proc. Int. Symp. on Wearable Computers (ISWC 2003), pp. 110–117, 2003.

[4] D. Wagner and D. Schmalstieg: "First steps towards handheld augmented reality,", Proc. Int. Symp. on Wearable Computers (ISWC 2003), pp. 21–23, 2003.

[5] M. Möhring, C. Lessig and O. Bimber: "Video see-through ar on consumer cell-phones,", Proc. Int. Symp. on Mixed and Augmented Reality (ISMAR 2004), pp. 252–253, 2004.

[6] R. Cipolla, D. Robertson and B. Tordoff: "Image-based localization,", Proc. Int. Conf. on Virtual Systems and Multimedia (VSMM 2004), pp. 22–29, 2004.

[7] J. Sato, T. Takahashi, I. Ide and H. Murase: "Change detection in streetscapes from gps coordinated omni-directional image sequences,", Proc. Int. Conf. on Pattern Recognition (ICPR 2006), Vol. 4, pp. 935–938, 2006.

[8] L. Vacchetti, V. Lepetit and P. Fua: "Combining edge and texture information for real-time accurate 3d camera tracking,", Proc. Int. Symp. on Mixed and Augmented Reality (ISMAR 2004), pp. 48–57, 2004.

[9] E. Rosten and T. Drummond: "Fusing points and lines for high performance tracking,", Proc. Int. Conf. on Computer Vision (ICCV 2005), Vol. 2, pp. 1508–1515, 2005.

[10] I. Skrypnyk and D. G. Lowe: "Scene modelling, recognition and tracking with invariant image features,", Proc. Int. Symp. on Mixed and Augmented Reality (ISMAR 2004), pp. 110–119, 2004.

[11] M. Oe, T. Sato and N. Yokoya: "Estimating camera position and posture by using feature landmark database,", Proc. Scandinavian Conf. on Image Analysis (SCIA 2005), pp. 171–181, 2005.

[12] T. Sato, S. Ikeda and N. Yokoya: "Extrinsic camera parameter recovery from multiple image sequences captured by an omni-directional multi-camera system,", Proc. European Conf. on Computer Vision, Vol. 2, pp. 326–340, 2004.

[13] C. Harris and M. Stephens: "A combined corner and edge detector,", Proc. Alvey Vision Conf., pp. 147–151, 1988.

[14] B. Triggs, P. McLauchlan, R. Hartley and A. Fitzgibbon: "Bundle Adjustment a Modern Synthesis," Proc. Int. Workshop on Vision Algorithms, pp. 298–372, 1999.

[15] S. Ikeda, T. Sato and N. Yokoya: "Camera recovery of an omnidirectional multi-camera system using gps positions,", Proc. First Korea-Japan Joint Workshop on Pattern Recognition, pp. 91–96, 2006.

[16] D. G. Lowe: "Distinctive image features from scale-invariant keypoints,", Int. Journal of Computer Vision, Vol. 60, No. 2, pp. 91–100, 2004.

[17] K. Mikolajczyk and C. Schmid: "Scale & affine invariant interest point detectors,", Int. Journal of Computer Vision, Vol. 60, No. 1, pp. 63–86, 2004.